Title: Stem canker caused by *Phomopsis spp*. induces changes in polyamine levels and chlorophyll fluorescence parameters in pecan leaves

Guillermo Martin Mantz[1+], Franco Ruben Rossi[1+], Pablo Esteban Viretto[2], María Cristina Noelting[3], Santiago Javier Maiale[1]*

[1]Instituto Tecnológico de Chascomús (INTECH), Consejo Nacional de Investigaciones Científicas y Técnicas (CONICET)-Universidad Nacional de San Martín (UNSAM), Int. Marino Km 8, Chascomús, Provincia de Buenos Aires, Argentina

[2]Estación Experimental Agropecuaria Valle Inferior del Río Negro (EEA)-Instituto Nacional de Tecnología Agropecuaria (INTA), Valle inferior Río Negro, RN 3 Km 971, Pcia. RN, Argentina

[3]Instituto Fitotécnico de Santa Catalina (IFSC), Universidad Nacional de La Plata (UNLP), Garibaldi 3400, Lavallol, Provincia de Buenos Aires, Argentina

[+]Both authors contributed equally to this work

*Corresponding author: santiagomaiale@hotmail.com

Keywords: pecan, *Phomopsis*, polyamines, chlorophyll fluorescence, proline

ABSTRACT

Pecan plants are attacked by the fungus *Phomopsis spp.* that causes stem canker, a serious and emerging disease in commercial orchards. Stem canker, which has been reported in several countries, negatively affects tree canopy health, eventually leading to production losses. The purpose of this study was to inquire into the physiology of pecan plants under stem canker attack by *Phomopsis spp*. To this end, pecan plants were inoculated with an isolate of *Phomopsis spp.* and several parameters, such as polyamines, proline, sugars, starch, chlorophyll fluorescence and canopy temperature were analysed. Under artificial inoculation, a high disease incidence was observed with symptoms similar to those in plants showing stem canker under field conditions. Furthermore, the infected stem showed dead tissue with brown necrotic discolouration in the xylem tissue. The free polyamines putrescine, spermidine, and spermine were detected and their levels decreased as leaves aged in the infected plants with respect to the controls. Chlorophyll fluorescence parameters, such as Sm, ψEO, and QbRC decreased under plant infection and therefore the K-band increased. Canopy temperature and proline content increased in the infected plants with respect to the controls while sugar content decreased. These data suggest that stem canker caused by *Phomopsis spp.* induces physiological changes that are similar to those observed in plants under drought stress. To our knowledge, this is the first study that documents the physiological and biochemical effects derived from pecan-*Phomopsis* interaction.

1 INTRODUCTION

The pecan tree (*Carya illinoinensis* (Wangenheim) K. Koch) produces seeds with high nutritional value and medicinal properties (Atanasov *et al*., 2017). It is native to North America (USA and Mexico) and is cultivated not only in the area of origin but also in many other countries in the temperate zone. Pecan plants are continuously exposed to different environmental stresses like pathogen attacks which cause a significant economic impact in the agricultural industry and lead to yield losses. Pecan canker was originally detected in Pima County (Arizona, USA) and was reported to be caused by *Cytospora spp.* (Hine *et al*., 1969), affecting scaffolds and other branches in two- and three-year-old plants. In this first approximation, Hine *et al*. observed that superficial lesions, such as those caused by low winter temperatures or sunburn in summer, are necessary to allow the fungal pathogen to enter host tissues and concluded that disease severity is genotype-dependent. Two types of Shoot Dieback Maladies (SDM) of pecan were further found to adversely affect tree canopy health in early spring and early summer in the USA pecan belt region. *Phomopsis spp.* and *Botryosphaeria spp.* were found to be the causal agents of SDM in 14 cultivars evaluated, representing 89% and 40% of the isolates, respectively (Reilly *et al*., 2010). Decline and mortality of hickory species belonging to the *Carya* genus (e.g., Shagbark and Bitternut) have been linked to *Ceratocystis smalleyii*, *Fusarium solani*, and *Phomopsis spp.* (Juzwik *et al*., 2008). The symptoms reported by Juzwik *et al*. included sunken small stem canker associated with *Ceratocystis* and *Fusarium* species and galls on the stem and branch associated with *Phomopsis spp*. Of the isolates documented in Juzwik *et al.*'s study, four were morphologically identical to those described as *Phomopsis spp.* and two of them matched in the GenBank database with *P. amygdale* and *Diaporthe helianthi*.

In Argentina, several diseases are known to affect the growth and development of pecan orchards, such as scab caused by *Venturia effusa* (ex-*Cladosporium caryigenum*) (Mantz *et al*., 2008), anthracnose on the pecan shuck and leaves caused by *Colletotrichum gloeosporioides* (Mantz *et al*., 2010) and nut pink mould caused by *Trichothecium roseum* (Mantz *et al*., 2009). All the latter have been recorded in the Pampas plains from central Argentina under temperate and moist weather conditions. A new disease whose causal agent was isolated from Pawnee cultivar has been recently recorded in Argentinean pecan orchards. It affects both the stems and branches and is typically characterised by canker symptoms. It was reported to belong to the genus *Phomopsis spp.* (Noelting *et al*., 2016).

Phomopsis is the asexual state of *Diaporthe* contains more than 900 species with broad hosts range and worldwide distribution, and the taxonomy of this fungus is constantly evolving (Udayanga *et al*., 2011, Gomes *et al*., 2013). Although *Diaporthe* is preferred to name this group of fungi, as in this work the anamorph was used, henceforth *Phomopsis* will be used to refer to this pathogen.

The symptoms include sunken and elongated lesions, particularly 0.5 to 1 cm long cankers mainly in the branches at the level of the neck or in the area of rootstock-scion union. These lesions are characterised by the presence of dark structures corresponding to fungus fruiting bodies (pycnidia). Cankered plants are characterised by bark sloughing and twig or branch death. These symptoms have been observed with high incidence and severity in numerous cultivars, such as Colby, Starking hardy giant, Desirable, Stuart, Lucas, Hirschi, and Pawnee, in the southern Argentinean Pampean region (Mantz, personal observation).

Under pathogen attack, plants use a wide variety of physical and chemical barriers derived from infection (Grant and Lamb, 2006). Polyamines (Pas) are one of these chemical barriers related to plant defence. They are natural aliphatic polycations essential for most organisms. At physiological pH, Pas are positively charged and therefore interact with anionic molecules, such as proteins, phospholipids, and nucleic acids. Diamine putrescine (Put), triamine spermidine (Spd), and tetramine spermine (Spm), which are the most abundant polyamines in plants (Bagni and Tassoni, 2001), are molecules involved in key processes, such as growth, development, morphogenesis, embryogenesis, senescence, and response to abiotic and biotic stress like plant defence mechanisms (Kusano *et al*., 2008). During plant-microbe interaction, Pas undergo a remarkable change (Jiménez Bremont *et al*., 2014, Romero *et al*., 2018). In line with this, previous research has shown that Pas content and metabolism are augmented in plants under pathogen attack independently of whether the pathogen infection strategy is via biotrophic or necrotrophic interactions (Walters, 2003; Jiménez Bremont *et al.* 2014; Romero *et al*. 2018). It has also been demonstrated that phytopathogens perturb the activity and functionality of photosystem and Pas levels (Vilas *et al*., 2018). Plants respond to biotic stress by adjusting their machinery to maintain photosynthetic activity. Once stress has overcome the acclimation capacity, permanent photoinhibition and inhibition of the electron transport chain occur (Perez-Bueno *et al*., 2019). Evidence from previous research (Hamdani *et al*., 2011) suggests a connection between Pas metabolism and photosynthetic activity. Exogenously added Spm may penetrate into the thylakoid membranes and interact with proteins and extrinsic polypeptides of the oxygen-evolving complex (OEC). Consequently, PSII activity could be preserved and protected from photoinhibition under high light stress by Spm (Hamdani *et al*., 2011).

120 In line with this, other authors found that Put is a stimulator of ATP biosynthesis while
121 Spd and Spm are efficient stimulators of non-photochemical quenching (Ioannidis and
122 Kotzabasis, 2007).
123 Taking all the above into account, the purpose of the present study was to inquire into
124 the physiology of pecan under stem canker attack by *Phomopsis spp*. To this end,
125 different physiological parameters, such as Pas levels, canopy temperature, and
126 chlorophyll fluorescence were analysed. Results from these analyses are –to our
127 knowledge– the first in reporting the physiological changes that occur in pecan leaves
128 as a result of infection with *Phomopsis spp*.
129

130 **2 MATERIALS AND METHODS**

131 **2.1 Biological material and growth conditions**

132 Experiments were carried out under ambient conditions at the campus of the *Instituto*
133 *Tecnológico de Chascomús* (INTECH), a research center depending on the National
134 Research Council (CONICET) and the Universidad Nacional de San Martín (UNSAM)
135 in Argentina. Meteorological data were taken from the Automatic Weather Station
136 located at the Experimental Station "Manantiales", a dependency of the *Instituto*
137 *Nacional de Tecnología Agropecuaria* (INTA) and the *Ministerio de Asuntos Agrarios*
138 in Buenos Aires province, Argentina (Supplemental Figure 1). The pecan plants, cv.
139 Pawnee, analysed herein were obtained from a local nursery, and the cultivar is the
140 same as that where the pathogen used in this study was isolated (Noelting *et al*., 2016).
141 The plants used as rootstock were produced from the pecan nut obtained from local
142 plant seedlings and they were grown in a 10 L pot for two years. Rootstocks were

143 grafted in autumn with buds from Pawnee, the scion was cultivated for one growing
144 season, and the following year they were used for the experiments herein described.
145 Control and inoculated plants were placed in a plastic pool and sub-irrigated with
146 rainwater twice a week.
147 *Phomopsis spp*. isolate number 1219, which corresponds to the isolate described by
148 Noelting *et al*. (2016), was obtained from the *Instituto de Botánica "Carlos Spegazzini"*
149 belonging to the *Universidad Nacional de La Plata*, in Argentina. The fungus was
150 routinely maintained on PDA agar at 22 ºC with a 12 h photoperiod to induce conidia
151 generation and was sub-cultured biweekly.
152

153 **2.2 Plant inoculations**

154 Inoculation was performed on 18 plants following Noelting *et al*. (2016). Briefly, in
155 November 2018, plugs of 0.5 cm in diameter of *Phomopsis spp.* growing actively on
156 PDA were used to inoculate pecan plants. Shoots growing during the year of the
157 experiment were used for inoculations, a 1 cm cut was made above the petiole insertion
158 with a scalpel and a mycelial plug was placed on the lesion. A piece of cotton wool
159 moistened in sterile water was placed on the mycelia plug to prevent mycelial
160 dehydration. Polyethylene film was used to hold the plug closely attached to the petiole.
161 Control treatments were carried out on other 18 plants following the same procedure
162 and on the same day as for the infected plants but using a PDA disk without mycelium.
163

164 **2.3 Free polyamine quantification**

165 Samples for Pas quantification were harvested on days 9 and 23 after inoculation (DAI).
166 At each time point, the fully developed leaflets of leaves located above the inoculation

point were detached and stored at -18 °C until use. Polyamines were analysed by derivatisation with dansyl chloride, separated in HPLC reverse phase, and detected by fluorescence according to Maiale *et al*. (2004) with modifications. Briefly, samples were powdered using a mortar and pestle precooled with N_2 liquid. Three hundred milligrams of plant powder were placed in a 1.5 ml microtube, and 1 mL of 5% $HClO_4$ was added, vortexed, and placed on ice for 30 min. Samples were subsequently centrifuged at 10000xg for 10 min, 60 µL of the sample were transferred to a microtube containing 60 µL of saturated Na_2CO_3, 6 µL of 0,1 mM 1,7 heptanodiamine (Htd) as internal standard, and 75 µL of 10 mg/mL dansyl-chloride in acetone. Samples were incubated at 70 ºC for two hours in the dark, the reaction was stopped by adding 20 µL of L-proline (100 mg/mL) and incubated for 15 min under the same conditions. Dansylated Pas were extracted with 200 µL of toluene, vacuum dried, and kept at -18 °C until quantification.

A HPLC binary pump (Waters 1525) attached to a C18 reverse-phase column 25x 4 mm Luna (2) (Phenomenex) and a diode array fluorescence detector (Waters 2475) were used in gradient protocols with acetonitrile (Act) and H_2O. Gradient protocols were used with a total time of 15 min following these steps: 0 to 4.5 min Act 70% - H_2O 30%, 4.5 to 5.5 min shifted to 100% Act, 5.5 to 9 min hold to 100% Act, 9 to 10 min shifted to Act 70% - H_2O 30% and 10 at 15 min maintain Act 70% - H_2O 30%. Dried samples were dissolved in 40 µL acetonitrile and injected in the HPLC through a 5 µL loop capacity. The fluorescence signal was detected at 415 nm excitation and 510 nm emission and integrated and processed using Breeze® software (Waters). A calibration curve with synthetic Pas was performed and Pas levels were calculated.

191 **2.4 Chlorophyll fluorescence fast-transient analysis**

192 Chlorophyll fluorescence was performed with a portable fluorometer (HandyPEA,
193 Hansatech Instruments, UK) on 0, 9, 16, and 23 DAI following Corigliano *et al*.
194 (2019), with modifications. Central leaflets of intact leaves above the inoculation point
195 were pre-darkened for 20 min before analysis using a leaf clip provided by the
196 manufacturer and they were subsequently exposed during 1 s to 3000 µmol photons
197 $m^{-2}s^{-1}$ (650 nm peak wavelength) with a dark interval of 500 ms and exposed during 1s
198 to 3000 µmol photons $m^{-2}s^{-1}$ again and chlorophyll-a fluorescence was recorded. The
199 fluorescence data were processed by PEA plus software (Hansatech Instruments, U.K.)
200 to obtain OJIP parameters. A summary of the OJIP parameters used in this study is
201 shown in Table 1.
202
203 **2.5 Canopy temperature measurements**
204 Canopy temperature was measured according to Rachoski *et al.* (2015) on 6, 10, 16, and
205 32 DAI using a thermal camera E-30 (FLIR, USA) with a resolution of 160 x 120 pixels
206 and a thermal sensitivity of 0.1 °C. The camera was calibrated at 2 metres, 20 °C
207 ambient temperature, 80% relative humidity, and an emissivity of 0.98. Thermographic
208 pictures were analysed with the ThermaCam Research PRO (FLIR, USA) software.
209
210 **2.6 Free sugar, starch, and proline determination**
211 Free sugars and starch were determined using the anthrone assay according to
212 Corigliano *et al*. (2019) with some modifications. Leaflets were homogenised in liquid
213 nitrogen. Sugars were extracted by adding 1 mL of EtOH 80% v/v to 10 mg of powder
214 and heated at 85 ºC for 30 min. The samples were subsequently centrifuged at 10000

rpm for 10 min, and the supernatant was transferred to a clear tube. This procedure was repeated three times and the supernatant was pooled. The pellet was dried and 100 µL of $HClO_4$ 35% were added and shaken in a vortex for 15 min and centrifuged for 10 min at 10000 rpm for starch solubilisation. Ethanolic or perchloric extract (6 µL) was mixed with 54 µL of distilled water, 240 µL of anthrone reagent (200 mg/mL in H_2SO_4 72%), and incubated at room temperature for 5 min. The total sugar and starch content was calculated by reading the absorbance at 630 nm in a microplate reader (BioTek Synergy H1. VT, USA) using a calibration curve performed with glucose.

Proline content was determined following Babuin *et al*. (2016). Briefly, powdered leaflet samples (250 mg FW) were placed in a 2 ml microtube and boiled in 1 mL of distilled water for 30 min. Samples were centrifuged at 10000 rpm for 10 min, 180 µL of supernatant were transferred in a 2 mL microtube containing 180 µL of sodium citrate buffer (0.2 mol/L at pH 4.6) and 720 µL of 1% ninhydrin solution in acetic acid: water (60:40) and boiled at 96 ºC for 1 h. Microtubes were subsequently cooled on ice, and proline was extracted with 720 µL of toluene by shaking in a vortex for 30 sec. The organic phase was read in a spectrophotometer at 520nm and a calibration curve with synthetic proline was constructed. Free sugar, starch, and proline content were determined on 9 and 23 DAI.

Dry weight was determined on 9 and 23 DAI by drying the leaflets in an oven at 70 °C and weighing up to constant weight. The biochemical data corresponding to Pas, proline, sugar, and starch were expressed on a dry weight basis.

3 RESULTS

3.1 Disease symptoms

The fungus strain used in this work was isolated from the pecan production zone of southern Argentina and its ITS sequence was previously deposited in the GenBank (accession Nº 359871).

Using the Mycobank database, it was possible to observe that *Phomopsis spp.* showed high pairwise similarity values with two *Diaporthe spp*. species, reaching 99.42 in each case, and with *D. helianthi* and *D. infecunda*, reaching values of 99.226 and 99.156, respectively. A phylogenetic tree was constructed with a Mega 6.06 software (Supplemental Figure 2) but no clear information could be obtained, *D. helianthi*, *D. infecunda*, and *D. middletoni* being the most related species. Further thorough research studies are necessary to determine the correct taxonomy of *Phomopsis spp.*

Inoculation was carried out in spring under ambient conditions. Control plants showed no visible symptoms of disease throughout the experimental period whereas typical stem canker symptoms were observed in almost all the infected plants, except for three plants in which infection was not successful. The latter were therefore not considered in subsequent analyses. These symptoms consisted of tissue necrosis in the inoculation zone with formation of small cankers. Under the microscope, the transversal section of the shoot on 24 DAI above the infection point showed a dark brown colour in the xylem tissue, while control plants showed no symptoms (Figure 1A-B). Black pycnidia were observed on the dead tissue of the inoculated plant cankers (Figure 1D). The macroscopic symptoms and signs were morphologically identical to those already reported in pecan and different plant species infected with *Phomopsis spp*. (Uddin *et al*., 1997; Reilly *et al.*, 2010; Noelting *et al*., 2016).

263

264 **3.2 Changes in free polyamine levels**

265 The changes that occurred in free Pas contents from pecan plants infected with
266 *Phomopsis spp.* at different times were analysed. On 9 DAI it was observed that the
267 most abundant Pas in the control pecan leaflets were Spd, followed by Spm and Put
268 with 56%, 28%, and 16%, respectively (Figure 2 and Supplemental Figure 3) and that
269 the levels of the three Pas detected in the infected plants were the same as those
270 observed in the control ones. The levels of Spd and Put were observed to decrease over
271 time in the control and infected plants, whereas Spm was found to remain constant. Put
272 content on 9 DAI vs. 23 DAI showed a decrease of 68% and 81% in the control and
273 infected plants, respectively. Spd content in the control plants on 9 DAI vs. 23 DAI
274 underwent a decrease of 28% and 40% in the control and infected plants, respectively.
275 Finally, Spm content in the control plants showed an increase of 19% while it
276 maintained a constant value on 9 and 23 DAI. However, on 23 DAI Spm levels showed
277 a significant decrease in the infected plants with respect to those in the control plants.
278 Total Pas levels, therefore, showed a tendency to decrease over time, such a decrease
279 being significant in the infected plants with respect to the controls (Figure 3).

280

281 **3.3 Measurement of chlorophyll a fluorescence transient parameters**

282 Photosynthesis is an integral part of plant metabolism and is extremely sensitive to
283 different stresses. In this respect, pathogenic infection often produces complex changes
284 in the host□s photosynthetic apparatus which can be estimated by fluorescence
285 measurements. In this work, fast transient chlorophyll a fluorescence was measured and
286 an OJIP analysis was performed. Based on the data collected, normalised fluorescence

curves were constructed. They showed a differential behaviour between the control and the infected plants. On 9 DAI the O-J and I-P steps of the infected plants showed differences with respect to those of the control plants, on 16 DAI the steps I-P and on 23 DAI the steps O-J showed a differential value between the control and infected plants (Supplemental Figure 4). At 0 time of inoculation, the control and infected plants did not show any significant differences in PIabs, Sm, Fv/Fm, and ψEO parameters. Nonetheless, these parameters were altered over the infection time course, and those particularly related to the health functionality of PSII were remarkably deteriorated (Figure 4E, 4F). Sm, ψEO, and PIabs parameters decreased along the experiment in the infected plants, yielding values of 88.9%, 91.3%, and 77.5% with respect to the controls on 23 DAI (Figure 4 B, 4C, and 4D). However, only ψEO and Sm showed a significant difference on 23 DAI.

Other OJIP parameters, namely DIo/CSo, ABS/RC, DIo/RC, and TRo/RC, increased in the infected plants with respect to the control plants (Supplemental Figure 5). In addition, differential Woj showed an increase in the K-band between the infected and control plants along the experiments, and the RC fraction that reduced QB showed a significant decrease in the infected plants on 23 DAI with respect to the controls (Figure 5A).

Furthermore, PIabs components, a multicomponent parameter related to energy conservation from photons absorbed by PSII to reduction QB (Table 1) showed a heterogeneous behaviour with RC/ABS tending to be less heterogeneous over time (Supplemental Figure 6).

3.4 Thermographic measurements of pecan plants

Leaf temperature is a consequence of the energy balance that includes the energy input of solar radiation and ambient heat and energy loss, such as, scattered light, heat loss, and transpired water. Pathogens may modify the values of these parameters when they infect plants (Bernard *et al*., 2013). For this reason, thermography becomes a useful tool to provide information on the transpiration of leaves attacked by a pathogen, especially in the early stages of pathogenesis when either symptom are not yet visible, or the infected area is small.

Plants inoculated with *Phomopsis spp.* showed an increase in canopy temperature which was measured with an infrared thermal camera (Figure 6). Although an increasing trend could –in fact– be observed in canopy temperature in the infected plants compared to the controls over the data collection time period in all the studied times (6-32 DAI), only on 16 DAI did the increase in temperature show significant differences.

3.5 Effects of *Phomopsis spp.* infection on free sugars, starch, and proline content

To study the levels of some organic solutes associated with different stressful conditions, free sugars, starch, and proline were measured in leaflets of pecan plants infected with *Phomopsis spp.* on 9 and 23 DAI. No significant differences were observed in free sugar or starch content at the two measurement times (Supplemental Figure 7). However, slightly higher levels of free sugars were observed in the control plants at both times analysed (17.42 and 14.19 vs. 16.95 and 13.25 mg of glucose eq. / 100mgDW in the control and infected plants, respectively) while starch values showed slightly higher values in the infected plants with respect to the controls (5.36 and 2.87

vs 6.05 and 3.40 mg glucose eq./100mgDW for the control and infected plants, respectively).

Proline content showed a strong increase on 9 and 23 DAI in the infected plants with respect to the control plants. On 9 DAI, proline levels showed an increase of 48% (Figure 7A) and 17.5% on 23 DAI (Figure 7B). No differences in dry weight content were observed in none of the treatments along the experiments performed (Supplemental Figure 8).

4 DISCUSSION

Pecan plants, like other cultivated plant species, are continuously exposed to potential production constraints which derive from a heterogeneous set of factors or agents that adversely affect pecan nut production, causing significant negative impact in the agricultural industry. Among these potential agents is the dieback which is associated with limb cankers. This complex and pernicious disease which causes dryness and falling branches is caused by *Phomopsis spp.* or by a fungal complex formed by *Phomopsis spp.* and *Botryosphaeria spp.* (Reilly *et al*., 2010). In the present work, we observed typical symptoms of stem canker in plants of pecan cv. Pawnee, artificially inoculated with *Phomopsis spp.* (Figure 1). These symptoms were identical to those previously reported in pecan plants in the southern Pampean region in Argentina (Noelting *et al*., 2016; Mantz personal observation). In this area, *Phomopsis spp.* (anamorphic state of *Diaporthe)* has been identified as the causal agent of cankers in limbs and dieback in branches in many cultivars in a pecan orchard.

According to the mechanism of infection, phytopathogenic fungi are classified into three broad categories, namely necrotrophic, biotrophic, and hemibiotrophic.

Necrotrophic fungi kill host cells before colonising them and they can grow and sporulate on dead tissue. In contrast, biotrophic fungi require living host tissue to survive as they feed on nutrients extracted directly from the living cell cytoplasm. Hemibiotrophic pathogens are initially biotrophic but become necrotrophic in a later stage (usually at the spore production stage) (Précigout *et al*., 2020). Taking this classification into account, the majority of *Phomopsis* species are thought to be hemibiotrophic (Udayanga *et al*., 2011). In our study, the symptoms of infection produced by *Phomopsis* were found to be compatible with those resulting from hemibiotrophic infection. The appearance of these symptoms was preceded by an asymptomatic post-inoculation period after which the proper symptoms of the disease emerged in the form of stem cankers.

Plants respond to pathogen attack by inducing the production of myriad proteins and metabolites. When such responses are triggered, Pas levels undergo remarkable changes. Evidence demonstrates that plants use polyamine biosynthetic pathway and oxidative catabolism as a defence mechanism against pathogens. Results from the present study demonstrate that the Pas found in pecan leaves correspond to those that are most abundant in the majority of plants, namely Put, Spd, and Spm (Supplemental Figure 2). In line with this, the free Pas levels measured in pecan leaflets in the present study showed similar values (Figure 2) to those found in other plant species, such as rice seedling leaves (Maiale *et al*., 2004), soybean hypocotyls (Campestre *et al.*, 2011), tobacco and corn seedling (Marina *et al*., 2008, Rodriguez-Kessler *et al*., 2008) and tomato leaves (Vilas *et al*., 2018). Previous studies on Pas content in woody plant species (Bartolini *et al*., 2009; Mirsoleimani and Shahsavar 2018; Liu and Moriguchi 2007; Rey *et al*., 1994) revealed that free total Pas levels ranged from 300 to 430

382 nmol/grFW in hazelnut leaves, from 500 to 1000 nmol/grFW in malus seedlings, from
383 437 to 600 nmol/grFW in peach flowers, and from 187 to 477 in nmol/grsFW in
384 Kinnow mandarin leaves. In all these plants, only Put, Spd, and Spm were detected and
385 the values corresponding to the three of them coincided with those reported in fresh
386 weight in the present study. In addition, although the Pas levels in the pecan leaves
387 analysed in the present study were found to be lower than those in the above-mentioned
388 woody plant species, they were in the same range (Figure 3A). Total free Pas levels
389 were observed to decrease over time as leaves aged (Figure 3A) in agreement with
390 observations documented in hazelnut and mandarin leaves (Rey *et al*., 1994,
391 Mirsoleimani and Shahsavar 2018). Further research showed that whereas Pas levels
392 increased in hazelnut trees after severe pruning as an indicator of juvenility and vigour,
393 they decreased in not pruned hazelnut trees, thus indicating ageing and senescence (Rey
394 *et al*., 1994).
395 Polyamine metabolism in plants infected by pathogens usually varies significantly
396 depending on plant species and pathogen nature. Findings from previous research
397 showed that Pas levels and the activity of polyamine metabolic enzymes are increased
398 in infected tissues during microbial colonisation, which seems to be independent of the
399 pathogenic attack mechanism (Jimenez-Bremont *et al*., 2014). In contrast, findings from
400 the present study indicated a gradual decrease in Put, Spd, and Spm levels in pecan
401 leaves from the infected plants with respect to the controls. In this respect, previous
402 research has shown that in some pathosystems Pas levels increase significantly
403 compared to their controls for a short period of time after which they return either to
404 initial or even lower levels as was observed for example in *Puccinia hordei* - Barley
405 interaction and *Puccinia graminis* - wheat interactions (Greenlands and Lewis 1984,

406 Foster and Walters 1992). In tobacco plants inoculated with *Peronospora tabacina*,
407 *Alternaria tenuis*, *Erysiphe cichoracearum*, *Pseudomonas tabaci*, and tobacco mosaic
408 virus, Pas levels were found to be lower than those in controls (Edreva, 1997).
409 Therefore, taking into account the above-mentioned findings, it appears to be prudent
410 not to discard the possibility that Pas levels increase at shorter times than those
411 evaluated in this work. On the other hand, comparative analyses between tolerant and
412 susceptible cultivars have shown variations in the Pas levels of plant species. In general,
413 cultivars tolerant to a certain pathogen compared to susceptible cultivars have been
414 observed to show a higher increase in Pas (Marini *et al*., 2001, Romero *et al*., 2018).
415 Given this scenario, it is prudent not to discard the possibility that the Pas levels
416 analysed in the present study are due either to a tolerant cultivar or to a low virulent
417 isolate of the pathogen.
418 Finally, the decrease in Pas levels observed in infected pecan leaves in the present study
419 could be due either to a decrease in the synthesis rate or to an increase in catabolism,
420 including a remobilisation of Pas to other tissues. For example, tobacco plants attacked
421 by the necrotrophic fungus *Sclerotinia sclerotiorum* showed an increase in Put and Spm
422 levels in the apoplast (Marina *et al*., 2008), which was associated to the catabolism of
423 Pas that ends up generating reactive oxygen species and thus collaborating with the
424 death of tissues, which is what is required by this type of pathogen. It was also observed
425 that the addition of Pas to infected tissues increases necrosis (Marina *et al*., 2008).
426 Transversal cuts in the limb region of *Phomopsis spp.*-infected pecan plants showed
427 dark brown spots in the xylem zone with abundant dead tissue that could accelerate
428 senescence in the leaves (Figure 1B). Senescence has been described as a process
429 associated with a decrease in Pas content (Sobieszczuk-Nowicka *et al*., 2019). In our

study, due to the hemibiotrophic nature of *Phomopsis*, a typical pattern of necrotrophic infection was observed after several days post-inoculation, a process that could accelerate mechanisms associated with senescence and consequently modify the levels of Pas.

On the other hand, PSII functionality evaluated by OJIP analysis showed a significant decrease in Sm and ψEO on 23 DAI (Figure 4B, 4D). Sm parameters indicate the number of electron carriers per electron carrier chain, whereas ψEO is the probability that trapped exciton moves an electron into the electron chain beyond QA and represents the energy of the electron transport about the energy trapped (Stirbet and Govindjee, 2011). These data indicate a decrease in the bulk in the electron carriers and a degree of inhibition in the step from QA reduced to QB reduction. At the same time, the QB reducing centre decrease on 23 DAI and the K-band (Woji-Wojc) increase overtime during the experiments (Figure 5) indicated a poor electron transfer from OEC to P680 and showed a similar shape to that produced by DCMU poisoning (Chen *et al*., 2014).

The genus *Diaporthe* is known to produce a set of compounds with antimicrobial and phytotoxic activity (Udayanga *et al*., 2011). Although, *D. helianthi,* in particular, which is the causal agent of stem canker of sunflower, has been reported to produce the phytotoxin Phomozin (Mazars *et al.*, 1990), no reports have been found to date on the effect of this toxin on the PSII. Other authors showed the effect of *D. phaseolorum* methanolic extracts on the PSII activity of *Senecio occidentalis* and *Ipomoea grandifolia* (Moura *et al*., 2020) with PIabs decrease and inhibition in the QB reduction. As the anamorph *Phomopsis* was used in this work, the presence of toxins in diseased plants could be a subject for future research.

454 Previous research has demonstrated that whereas Pas of three and four amine groups,
455 like Spm and Spd, show photoprotection in isolated thylakoid membranes, Put or
456 methylamine have no effect on this mechanism. This photoprotection is due to the
457 polycationic nature of Spm that stabilises the conformation of PSII protein through
458 electrostatic interaction (Hamdani *et al*., 2011). In the present study, a significant
459 decrease of Spm and Spd was recorded on 23 DAI in the infected plants in agreement
460 with the deterioration of PSII functionality, thus indicating a possible connection
461 between Spm levels and photosynthetic activity which could lead to the hypothesis that
462 *Phomopsis* manipulates Pas metabolism for its benefit.
463 Sugar concentration is a good indicator of the plant energetic balance during plant-
464 fungus interaction (Nieva *et al*., 2019) and the decay of PSII functionality in infected
465 plants could be associated with lower photosynthetic activity and sugar content. In the
466 present study, both PSII functionality and sugar content were observed to decrease in
467 the infected plants (Supplemental Figure 7B) in agreement with data collected from
468 other plant fungus interactions, such as *Oidium heveae* - *Hevea brasiliensis*, *Botrytis*
469 *cinerea* - *Solanum lycopersicum*, and *Fusarium solani* - *Lotus tenuis* (Wang *et al*., 2014;
470 Berger *et al*., 2004; Nieva *et al*., 2019).
471 Furthermore, heat loss occurs via water evaporation which cools the canopy and
472 therefore the subsequent stomatal closure or water supply decrease elicits a leaf
473 temperature increase which could be interpreted as a stress indicator (Costa *et al*.,
474 2013). Pinter *et al*. (1979) found an increase in leaf temperature of 3 to 4 °C in
475 moderately diseased plants of sugar beet and cotton affected by root rot pathogen
476 infection. Other studies have reported similar relationships between pathogen attack to
477 the root system and leaf temperature increase (Tu and Tan 1985; Calderon *et al*., 2013),

478 and further research concluded that vascular damage or obstruction could be a cause of
479 the reduction of water supply to the leaves (Huang *et al*., 2020). In the same direction,
480 the augmented canopy temperature in pecan plants infected with *Phomopsis spp*. and
481 the necrotic xylem tissue in the zone of infection suggest that both events could be
482 related, and further research is necessary to clarify this relationship (Figure 1).
483 Proline contents increase under different stress types because this amino acid has
484 important roles as membrane structure stabiliser and reactive oxygen scavenger under
485 drought stress (Chun *et al*., 2018). Under mild drought stress, it was observed that
486 whereas proline contents show a significant increase, the relative water content shows
487 no changes, thus suggesting that this amino acid is more sensitive as an indicator of
488 drought stress in pecan leaves (Babuin *et al*., 2016). Taking this into account, the
489 augmented canopy temperature (Figure 6) and the accumulation of proline observed as a
490 consequence of infection in the present study (Figure 7) could be another indicator of
491 drought stress, as documented in pecan plants under restricted water supply (Babuin *et*
492 *al*., 2016).
493 Furthermore, whereas the shape of the K-band (Figure 5B) observed in the infected
494 pecan plants coincided with the shape of the K-band in plants with symptoms of
495 drought stress (Oukarroum *et al*., 2007), Abs/RC and DIo/RC increased in the infected
496 plants on 23 DAI in contrast to what occurred in the controls (Supplemental Figure 5) as
497 documented in rubber tree under drought stress (Falqueto *et al*., 2017). All in all, the
498 data collected in the present study suggest that the symptoms resulting from *Phomopsis*
499 *spp.* infection in pecan plants mimics those derived from drought stress. The
500 physiological effects observed in infected plants in the present study also coincide with
501 symptoms of twig and branch dieback in plants in the field.

As a concluding remark, it can be said that although there are still several unexplored niches, such as –among others– the potential presence of toxins as a result of *Phomopsis spp.* infection in pecan leaves and the effect of this pathogen on stomata regulation and water supply to the leaves, the findings from the present study make an important contribution to understanding the effects of stem canker caused by fungi of the genus of *Phomopsis* on pecan plant physiology.

Acknowledgements

This work was funded by a grant provided by CONICET (PIP0363-2013). This work is part of the specializing thesis in tree nuts of GMM.

Data availability statement

The data that support the findings from this study are available from the corresponding authors upon reasonable request.

REFERENCES:

Atanasov AG, Sabharanjak SM, Zengin G, *et al.*, 2018. Pecan nuts: A review of reported bioactivities and health effects. *Trends in Food Science and Technology* **71**, 246–257.

Babuin MF, Echeverria M, Menendez AB, Maiale SJ, 2016. Arbuscular Mycorrhizal Pecan Seedlings Alleviate Effect of Restricted Water Supply. *Hortscience* **51**, 212–215.

527 Bagni N, Tassoni A, 2001. Biosynthesis, oxidation, and conjugation of aliphatic
528 polyamines in higher plants. *Amino Acids* **20**, 301–317.

529 Bartolini G, Toponi MA, Pestelli P, 2009. Free polyamine variations in rooting of Vitis
530 rootstock 140 Ruggeri. *Advances in Horticultural Science* **23**, 113–117.

531 Berger S, Papadopoulos M, Schreiber U, Kaiser W, Roitsch T, 2004. Complex
532 regulation of gene expression, photosynthesis, and sugar levels by pathogen
533 infection in tomato. Physiologia Plantarum, **122**, 419-428.

534 Bernard F, Sache I, Suffert F, Chelle M, 2013. The development of a foliar fungal
535 pathogen does react to leaf temperature. *New Phytol*ogist **198**, 232-240.

536 Calderon R, Navas-Cortes J, Lucena C, et al, 2013. High resolution airborne
537 hyperspectral and thermal imagery for early detection of Verticillium wilt of olive
538 using fluorescence, temperature, and narrow-band spectral indices. *Remote sensing*
539 *of Environments*, **139**,231-245.

540 Campestre MP, Bordenave CD, Origone AC, *et al.*, 2011. Polyamine catabolism is
541 involved in response to salt stress in soybean hypocotyls. *Journal of Plant*
542 *Physiology* **168**, 1234–1240.

543 Chen S, Strasser RJ, Qiang S, 2014. In vivo assessment of the effect of phytotoxin
544 tenuazonic acid on PSII reaction centers. *Plant Physiology and Biochemistry* **84**,
545 10–21.

546 Chun C, Paramasivan M, Chandrasekaran M, 2018. Proline accumulation influenced by
547 osmotic stress in arbuscular mycorrhizal symbiotic plants. *Frontiers in*
548 *Microbiology* **9**, 2525.

549 Corigliano MG, Albarracín RM, Vilas JM, *et al.*, 2019. Heat treatment alleviates the
550 growth and photosynthetic impairment of transplastomic plants expressing
551 Leishmania infantum Hsp83-Toxoplasma gondii SAG1 fusion protein. *Plant*
552 *Science* **284**, 117–126.

553 Costa J, Grant O, Chaves M, 2013. Thermography to explore plant-environment
554 interactions. *Journal Experimental Botany*, **64** (13), 3937-3949.

555 Edreva A, 1997. Tobacco polyamines as affected by stresses induced by different
556 pathogens. *Biologia Plantarum* **40**, 317–320.

557 Falqueto AR, da Silva Júnior RA, Gomes MTG, Martins JPR, Silva DM, Partelli FL,
558 2017. Effects of drought stress on chlorophyll a fluorescence in two rubber tree
559 clones. *Scientia Horticulturae* **224**, 238–243.

560 Foster SA, Walters DR, 1992. Polyamine Concentrations and Activities of Ornithine
561 and Arginine Decarboxylase in Wheat Infected with the Stem Rust Fungus.
562 *Journal of Plant Physiology* **140**, 134–136.

563 Gomes PR, Glienke C, Videira SIR, Lombard L, Groenewald JZ, Crous PW, 2013.
564 Diaporthe: a genus of endophytic, saprobic and plant pathogenic fungi. *Persoonia*
565 **31**, 1-41.

566 Grant M, Lamb C, 2006. Systemic immunity. *Current Opinion in Plant Biology* **9**, 414–
567 420.

568 Greenlands AJ, Lewis DH, 1984. Amines in barley leaves infected by brown rust and
569 their possible relevance to the formation of "green islands." *New Phytologist* **96**,
570 283–291.

571 Hamdani S, Gauthier A, Msilini N, Carpentier R, 2011. Positive charges of polyamines
572 protect PSII in isolated thylakoid membranes during photoinhibitory conditions.
573 *Plant and Cell Physiology* **52**, 866–873.

574 Hine R, Wheeler J, Clark E, 1969. New Canker disease found in pecans. Progressive
575 Agriculture 21 (5), 17.

576 Huang Y, Ren Z, Li D, Liu X, 2020. Phenotypic techniques and applications in fruit
577 trees: a review. *Plant Methods*, **16**, 107.

578 Ioannidis NE, Kotzabasis K, 2007. Effects of polyamines on the functionality of
579 photosynthetic membrane in vivo and in vitro. *Biochimica et Biophysica Acta -*
580 *Bioenergetics* **1767**, 1372–1382.

581 Jiménez-Bremont JF, Marina M, Guerrero-González M de la L *et al.*, 2014.
582 Physiological and molecular implications of plant polyamine metabolism during
583 biotic interactions. *Frontiers in Plant Science* **5**, 1–14.

584 Juzwik J, Haugen L, Park JH, Moore M, 2008. Fungi associated with stem cankers and
585 coincidental scolytid beetles on declining hickory in the upper Midwest.
586 *Proceedings of the 16th central hardwood forest conference*, 476–482.

587 Kusano T, Berberich T, Tateda C, Takahashi Y, 2008. Polyamines: Essential factors for
588 growth and survival. *Planta* **228**, 367–381.

589 Liu JH, Moriguchi T, 2007. Changes in free polyamines and gene expression during
590 peach flower development. *Biologia Plantarum* **51**, 530–532.

591 Maiale S, Sánchez DH, Guirado A, Vidal A, Ruiz OA, 2004. Spermine accumulation
592 under salt stress. *Journal of Plant Physiology* **161**, 35–42.

593 Mantz G, Maiale S, Rollán C, Ronco L, 2009. Occurrence of scab disease of pecan
594 caused by Cladosporium caryigenum in Argentina. *Plant Pathology* **58**, 802.

595 Mantz G, Minhot R, Morrelli G, Maiale S, 2010. First report of Colletotrichum
596 gloeosporioides causing pecan anthracnose in Argentina. *Journal of Plant*
597 *Pathology* **92**, 544.

598 Mantz G, Rollán C, Ronco L, Maiale S, 2009. First report of pink mold on pecan nuts in
599 Argentina. *Journal of Plant Pathology* **91**, 238.

600 Marina M, Maiale SJ, Rossi FR, *et al.*, 2008. Apoplastic polyamine oxidation plays
601 different roles in local responses of tobacco to infection by the necrotrophic fungus
602 Sclerotinia sclerotiorum and the biotrophic bacterium Pseudomonas viridiflava.
603 *Plant Physiology* **147**, 2164–2178.

604 Marini F, Betti L, Scaramagli S, Biondi S, Torrigiani P, 2001. Polyamine metabolism is
605 upregulated in response to tobacco mosaic virus in hypersensitive, but not in
606 susceptible, tobacco. *New Phytologist* **149**, 301–309.

607 Mazars C, Rossignol M, Auriol P, Klaebe A, 1990. Phomozin, a phytotoxin from
608 Phomopsis helianthi, the causal agent of stem canker of sunflower. *Phytochemistry*
609 **29**, 3441–3444.

610 Mirsoleimani A, Shahsavar A-R, 2018. Changes of free polyamines in the leaves and
611 stems of Kinnow mandarin tree as affected by alternate bearing. *Journal of Plant*
612 *Process and Function* **6**.

613 Moura M, Lacerda J, Siqueira K, et al. 2020. Endophytic fungal extracts: evaluation as
614 photosynthesis and weed growth inhibitors. *Journal of Environmental Science and*
615 *Health, Part B*, **55**, 5, 470-476.

616 Nieva S, Vilas J, Garriz A, et al. 2019. The fungal endophyte Fusarium solani provokes
617 differential effects on the fitness of two Lotus species. Plant Physiology and
618 Biochemistry, **144**, 100-109.

619 Noelting MC, Mantz GM, Maiale SJ, Molina MC, 2016. Occurrence of Phomopsis sp.
620 causing cankers on pecan trees in Buenos Aires province, Argentina. *New Disease*
621 *Reports* **33**, 9.

622 Oukarroum A, Madidi S El, Schansker G, Strasser RJ, 2007. Probing the responses of
623 barley cultivars (Hordeum vulgare L.) by chlorophyll a fluorescence OLKJIP
624 under drought stress and re-watering. *Environmental and Experimental Botany* **60**,
625 438–446.

626 Pérez-Bueno ML, Pineda M, Barón M, 2019. Phenotyping Plant Responses to Biotic
627 Stress by Chlorophyll Fluorescence Imaging. Frontiers in Plant Science **10**, 1135.

628 Pinter P, Stanghellini M, Reginato R, et al, 1979. Remote detection of biological stress
629 in plants with infrared thermography. *Science*, **205**:585-87.

630 Précigout PA, Claessen D, Makowski D, Robert C, 2020. Does the Latent Period of
631 Leaf Fungal Pathogens Reflect Their Trophic Type? A Meta-Analysis of
632 Biotrophs, Hemibiotrophs, and Necrotrophs. Phytopathology **110**, 345-361

633 Rachoski, M., Gazquez, A., Calzadilla, P. *et al.* 2015. Chlorophyll fluorescence and
634 lipid peroxidation changes in rice somaclonal lines subjected to salt stress. *Acta*
635 *Physiol Plant* **37,** 117.

636 Reilly CC, Wood BW, Stevenson KL, 2010. Relationship of shoot dieback in pecan to
637 fungi and fruiting stress. *HortScience* **45**, 87–91.

638 Rey M, Diaz-sala C, Rodríguez R, 1994. Effect of repeated severe pruning on
639 endogenous polyamine content in hazelnut trees. *Physiologia Plantarum* **92**, 487–
640 492.

641 Rodriguez-Kessler M, Ruiz OA, Maiale S, Ruiz-Herrera J, Jiménez-Bremont JF, 2008.
642 Polyamine metabolism in maize tumors induced by Ustilago maydis. *Plant*
643 *Physiology and Biochemistry* **46**, 805–814.

644 Romero FM, Maiale SJ, Rossi FR, Marina M, Ruíz OA, Gárriz A, 2018. Polyamine
645 Metabolism Responses to Biotic and Abiotic Stress. *Methods in Molecular Biology*
646 **1694**, 37-49.

647 Rosskopf EN, Charudattan R, Shabana YM, Benny GL, 2000. Phomopsis
648 amaranthicola, a new species from Amaranthus sp. *Mycologia* **92**, 114–122.

649 Sobieszczuk-Nowicka Ewa, Paluch-Lubawa Ewelina, Mattoo Autar K., Arasimowicz-
650 Jelonek Magdalena, Gregersen Per L., Pacak Andrzej, 2019. Polyamines – A New
651 Metabolic Switch: Crosstalk with Networks Involving Senescence, Crop
652 Improvement, and Mammalian Cancer Therapy. *Frontiers in Plant Science* **10**, 859

653 Stirbet A, Govindjee, 2011. On the relation between the Kautsky effect (chlorophyll a
654 fluorescence induction) and Photosystem II: Basics and applications of the OJIP
655 fluorescence transient. *Journal of Photochemistry and Photobiology B: Biology*
656 **104**, 236–257.

657 Tun J, Tan C, 1985. Infrared thermometry for determination of root rot severity in
658 beans. *Phytopathology*, **75**, 840-844.

659 Uddin W, Stevenson K, PardoSchultheiss R, 1997. Pathogenicity of a species of
660 Phomopsis causing a shoot blight on peach in Georgia and evaluation of possible
661 infection courts. *Plant Disease*, **81**, 983–989

662 Udayanga D, Liu X, McKenzie EHC, Chukeatirote E, Bahkali AHA, Hyde KD, 2011.
663 The genus Phomopsis: Biology, applications, species concepts, and names of
664 common phytopathogens. *Fungal Diversity* **50**, 189–225.

665 Vilas JM, Romero FM, Rossi FR, *et al.*, 2018. Modulation of plant and bacterial
666 polyamine metabolism during the compatible interaction between tomato and
667 Pseudomonas syringae. *Journal of Plant Physiology* **231**, 281–290.

668 Walters DR, 2003. Polyamines and plant disease. *Phytochemistry* **64**, 97–107.

669 Wang L, Wang M, Zhang Y, 2014. Effects of powdery mildew infection on chloroplast
670 and mitochondrial functions in rubber tree. Tropical Plant Pathology, **39** (3), 242-
671 250.

672

673

674

675

676

677

678

679

680

681

682

683

684

685

686

687

688

689

690

691

692

693

694 Table 1: Chlorophyll fluorescence parameters analysed by OJIP test.

695 Technical fluorescence parameters

696

697 Ft = fluorescence at time t after onset actinic light
698 Fo = minimal fluorescence (all PSII RC are open)
699 F100 = fluorescence at time 100 µs
700 Fk = fluorescence at time 300 µs (K-step)
701 Fj = fluorescence at time 2 ms (J-step)
702 Fi = fluorescence at time 30 ms (I-step)
703 Fp = Fm = maximal fluorescence (all PSII RC are closed)
704 tFm = time (in ms) to reach Fm
705 Area = complementary area on the OJIP curve
706 Mo = 4. (F250 µs - Fo)/ (Fm - Fo) initial slope of the fluorescence transient
707 Vj = (Fj - Fo)/(Fm – Fo) = relative variable fluorescence at the J-step
708 Vi = (Fi-Fo)/ (Fm-Fo) = realtive variable fluorescence at the I-step
709 W100 = (F100 - Fo)/ (Fj – Fo) = fluorescence at F100 normalized by Vj
710 W300 = (Fk - Fo)/ (Fj – Fo) = fluorescence at Fk normalized by VJ
711 k = 4. (Ln (Fj – Fo)/ (Fj – Fk)) = rate constant of the exponential fluorescence rise
712 WE100 = 1 – (1-(2,718281828^ (-k . 0,05)) = theoretical exponential curve corresponding to unconnected
713 system
714 Cw = (WE100 - W100)/ (W100 . (1- WE100) = curvature constant of the hyperbole
715 Sm = Area/(Fm-Fo) normalized complementary area (related to the number of electron carriers per
716 electron carriers' chain or energy needed to close all RC)
717 N = turnover number of QA reduction events
718 Fo/Fm = kn/kp = relation between non-photochemical and photochemical quenching rate constant
719
720 Quantum efficiencies or probabilities
721 Tro/ABS = 1-Fo/Fm = Fv/Fm = φpo = maximum quantum yield of primary PSII photochemistry
722 ETo/TRo = ψeo = (1-Vj) = probability that trapped exiton move an electron into the electron chain
723 beyond QA
724 REo/ETo = (1-Vi)/ (1-Vj) = δeo = probabilities with wich an electron from QB is transferred until PSI
725 acceptors
726 REo/ABS = 1-Fi/Fm = φro = quantum yield of electron transport flux until the PSI electron acceptors
727
728 Phenomenological energy fluxes (per excited cross section - Cs)
729 ABS/Cs = Fo = absorption flux per Cs
730 Dio/Cs = (ABS/Cs) - (TRo/Cs) = disipation flux per Cs
731 TRo/Cs = φpo. (ABS/Cs) = trapped flux per Cs
732 ETo/Cs = φpo. Ψeo. (ABS/Cs) = electron transport per Cs
733 REo/Cs = (REo/ABS) . (ABS/Cs) = transport flux until PSI per Cs
734
735 Others parameters
736 RC/Cs = φpo. (Vj/Mo). (ABS/Cs) = QA reduction reaction center per Cs
737 RC/ABS = γ/ (1- γ) = φpo. (Vj/Mo) = QA reducing RC per PSII antenna Chlorophyll
738 PIABS = RC/ABS . φpo/ (1- φpo) . ψeo/ (1- ψeo) = performance index for energy conservation from
739 photons absorbed by PSII to reduction QB
740 P (conectivity) = (Cw . Fo)/((Fm – Fo). Fj)) = probability of connectivity between PSII units.

741

742

743

744 **Figure legends**

745

746 Figure 1: Transversal section of the stem above the point of infection on day 24 after

747 inoculation and view of the area inoculated. A and C- mock-infected plant; B and D-

748 plant inoculated with *Phomopsis spp*.

749

750 Figure 2: Polyamine content of putrescine (Put.), spermidine (Spd.), and spermine

751 (Spm.) in control leaflets of pecan leaves (white bar) and in leaflets of pecan leaves

752 infected with *Phomopsis spp.* (grey bar) on days 9 and 23 after inoculation. Data are

753 mean with SEM and t-tests were performed for each sampling time comparing control

754 plants and infected plants with a Graph Pad Prism®, ns-no significant; * $p \leq 0.05$; ** $p \leq$

755 0.01; *** $p \leq 0.0001$, n control: 16; n infected: 15.

756

757 Figure 3: Total polyamine content in control (white bar) and infected (grey bar) pecan

758 plants on days 9 and 23 after inoculation. Data are mean with SEM and t-tests were

759 performed for each sampling time comparing control plants and infected plants with a

760 Graph Pad Prism®, ns-no significant; * $p \leq 0.05$; ** $p \leq 0.01$; *** $p \leq 0.0001$, n control:

761 16; n infected: 15.

762

763 Figure 4: Chlorophyll a fluorescence parameters in leaflets of pecan control plants

764 (white bar) and infected plants (grey bar) on days 1, 9, 16, and 23 after inoculation. A-

765 Fv/Fm is the maximum quantum yield of primary PSII photochemistry; B- Sm is the

766 electron transport chain per reaction centre; C- Piabs is a performance index for energy

767 conservation from absorbed photons to reduction QB; D- ΨE_0 is the probability that a

768 trapped exciton moves an electron beyond QA; E- Fv/Fm, Sm, PIabs and ΨE0 values in
769 percentage, normalised and compared with values in the control plants on day 0; F-
770 Fv/Fm, Sm, PIabs and ΨE_0 values in percentage compared with values in the control
771 plants. Percentage in bars indicate the difference between the infected and control plants
772 at each measurement time. Data are mean with SEM and t-tests were performed for
773 each sampling time comparing control plants and infected plants with a Graph Pad
774 Prism®, ns-no significant; * p≤ 0.05; ** p≤ 0.01; *** p≤ 0.0001, n control: 16; n
775 infected: 15.
776
777 Figure 5: A- Fraction of the reaction centre that reduces QB in the controls (white bar)
778 and infected plants (grey bar) on days 0, 9, 16, and 23 after inoculation. B- K-band
779 (WojI-WojC) shown on days 0, 9, 16, and 23 after inoculation; insert Woj= $(Ft-F_0)/(Fj-$
780 $F_0)$ on the same day of measurement. Data are mean with SEM and t-tests were
781 performed for each sampling time comparing control plants and infected plants with a
782 Graph Pad Prism®, ns-no significant; * p≤ 0.05; ** p≤ 0.01; *** p≤ 0.0001, n control:
783 16; n infected: 15.
784
785 Figure 6: Canopy temperature in º C measured by thermography on days 6, 10, 16, and
786 32 after inoculation in control plants (white bars) and infected plants (grey bars).
787 Numbers above bars indicate differences in ºC between infected and control plants.
788 Data are mean with SEM and t-tests were performed for each sampling time comparing
789 control plants and infected plants with a Graph Pad Prism®, ns-no significant; * p≤ 0.05;
790 ** p≤ 0.01; *** p≤ 0.0001, n control: 16; n infected: 15.
791

792 Figure 7: Proline content in leaflets of pecan control plants (white bars) and of infected
793 plants (grey bars) on days 9 (A) and 23 (B) after inoculation. Data are mean with SEM
794 and t-tests were performed for each sampling time comparing control plants and
795 infected plants with a Graph Pad Prism®, ns-no significant; * $p \leq 0.05$; ** $p \leq 0.01$; ***
796 $p \leq 0.0001$, n control: 16; n infected: 15.
797
798 **Supplemental figure legends**
799
800 SF 1: Weather data: maximum temperature (black line), minimum temperature (grey
801 line) in º C, and RH (broken line) in percentage. Arrows indicate the sampling moment.
802 Dots indicate the moment at which canopy temperature was measured.
803
804 SF2: Genealogical Tree constructed with a MEGA 6.06 software using data taken from
805 the GeneBank. The *Phomopsis spp.* sequence (KU359781.1 MGM1) analysed in this
806 study was used together with the 28 sequences that showed the greatest similarity in the
807 GeneBank, the sequence MH042300 belonging to *Epicoccum nigrum* strain 180305 was
808 used as a reference.
809
810 SF 3: Polyamine chromatograms obtained in reverse phase HPLC. Standard is a mixture
811 of synthetic polyamines diamopropane, cadaverine, putrescine, heptanodiamine,
812 spermidine, and spermine. Control and inoculated chromatograms showed peaks of
813 putrescine, spermidine and spermine, and the internal standard heptanodiamine.
814

SF4: Normalised OJIP curves $(Ft-F_0)/(Fm-F_0)$ in control plants (black line) and infected plants (grey line) on days 0, 9, 16 and 23 after inoculation.

SF5: Spider plot of a group of parameters obtained via OJIP analysis on days 0 (A), 9 (B), 16 (C) and 23 (D) after inoculation.

SF6: Spider plot of another group of parameters obtained via OJIP analysis on days 0 (A), 9 (B), 16 (C) and 23 (D) after inoculation.

SF7: Glucose (A and C) and starch (B and D) on days 9 (A and B) and 23 (C and D) after inoculation in control plants (white bars) and infected plants (grey bars). Data are mean with SEM and t-tests were performed for each sampling time comparing control plants and infected plants with a Graph Pad Prism®. No significant differences were observed.

SF8: Dry weight content in leaflets of pecan control plants (white bars) and infected plants (grey bars) on days 9 (A) and 23 (B) after inoculation. Data are mean with SEM and t-tests were performed for each sampling time comparing control plants and infected plants with a Graph Pad Prism®, ns-no significant; * $p \leq 0.05$; ** $p \leq 0.01$; *** $p \leq 0.0001$, n control: 16; n infected: 15.

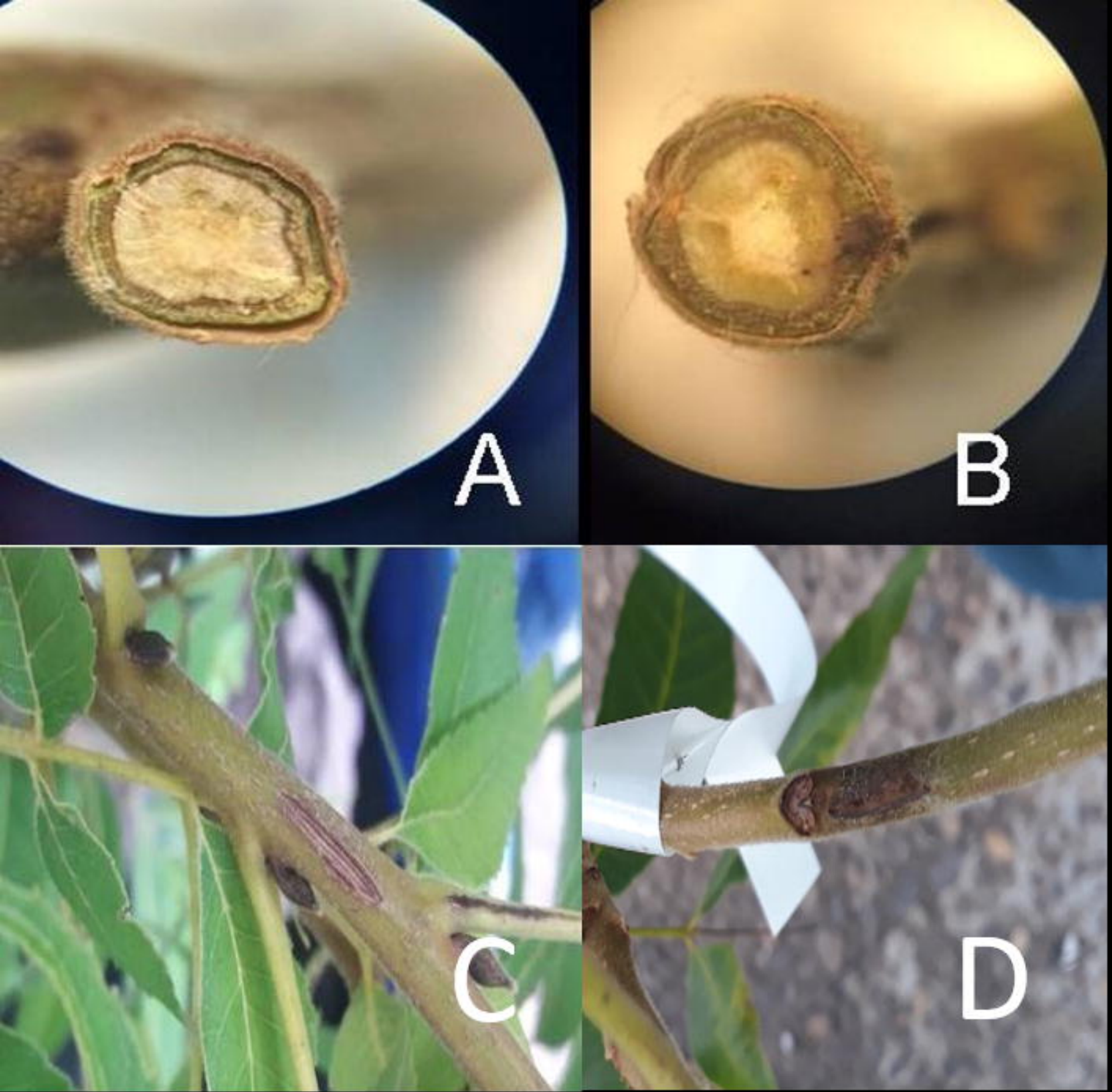
A
B
C
D

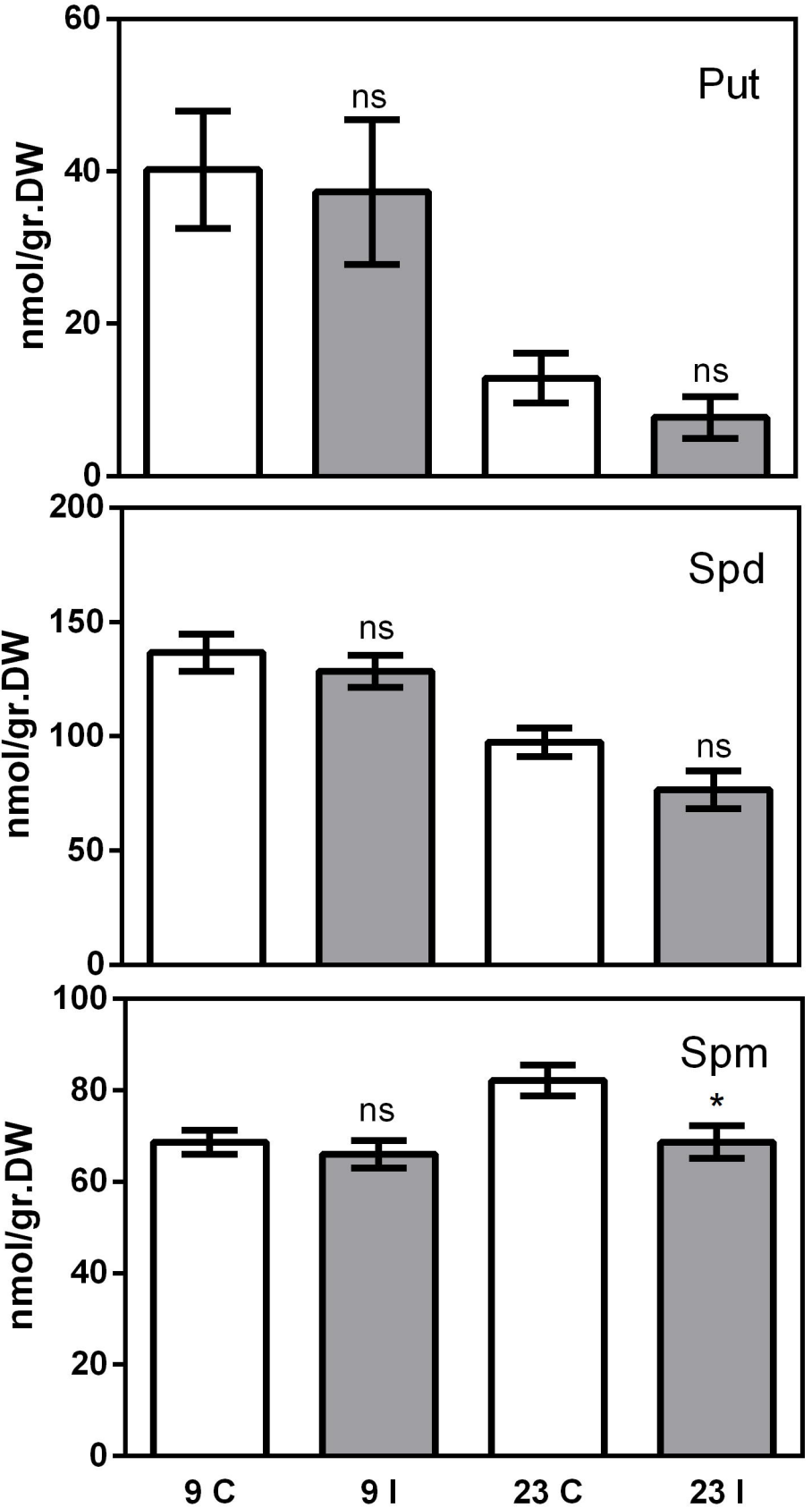
Put
Spd
Spm
nmol/gr.DW
60
40
20
0
200
150
100
50
100
80
60
40
20
ns
ns
ns
ns
ns
*
9 C
9 I
23 C
23 I

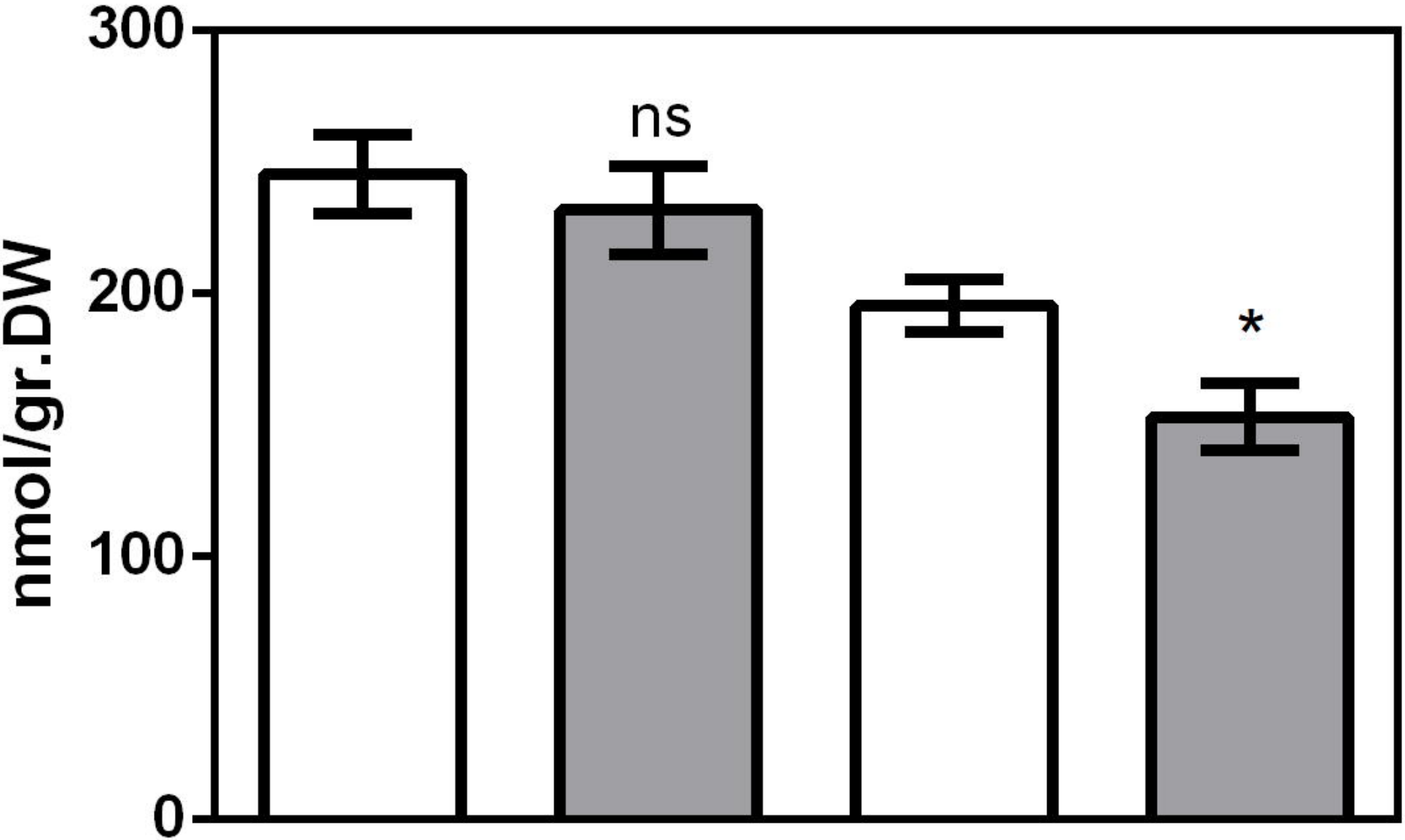
300
200
100
0
nmol/gr.DW
ns
*

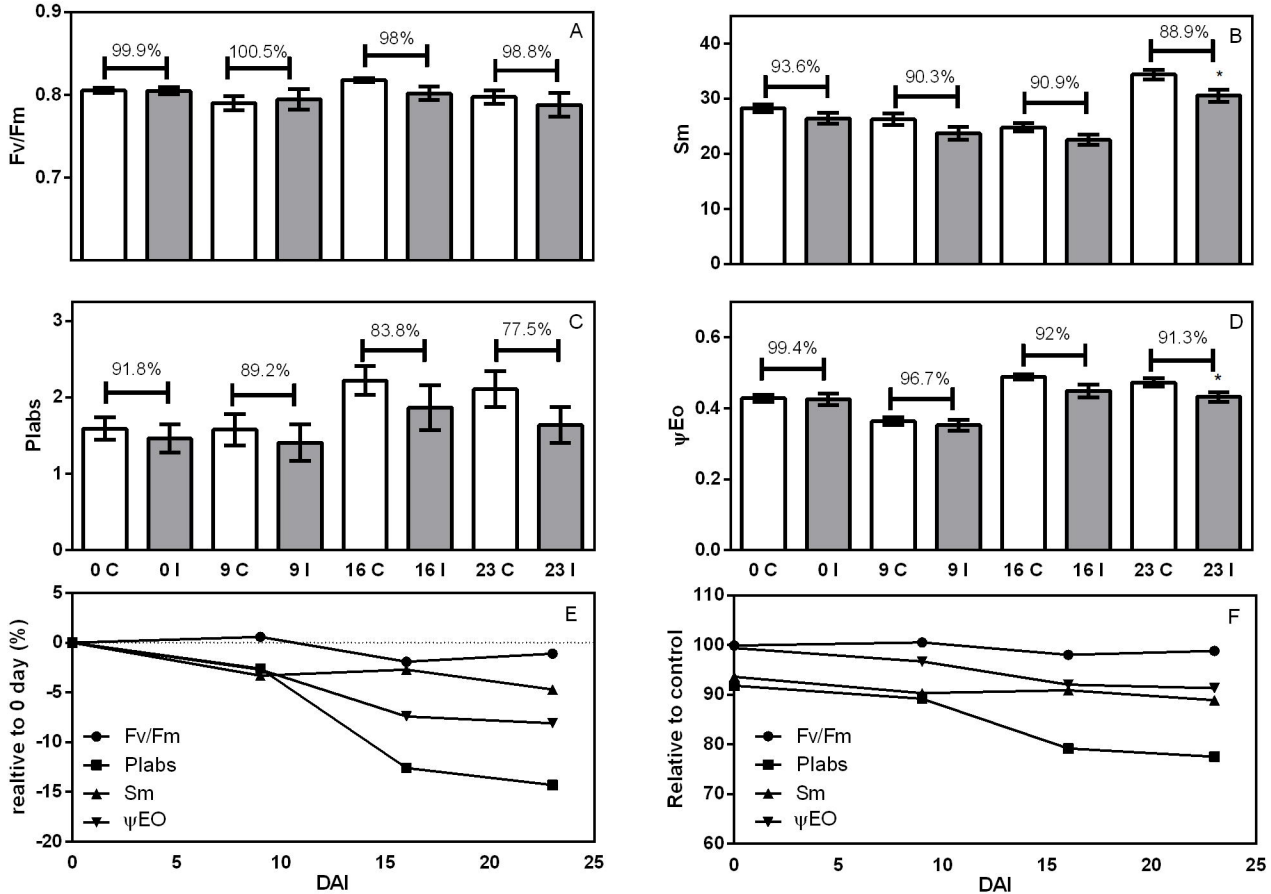
A
Fv/Fm
0.9
0.8
0.7
99.9%
100.5%
98%
98.8%
B
Sm
40
30
20
10
0
93.6%
90.3%
90.9%
88.9%
*
C
Plabs
3
2
1
0
91.8%
89.2%
83.8%
77.5%
0 C
0 I
9 C
9 I
16 C
16 I
23 C
23 I
D
ψEo
0.6
0.4
0.2
0.0
99.4%
96.7%
92%
91.3%
*
E
realtive to 0 day (%)
5
0
-5
-10
-15
-20
Fv/Fm
Plabs
Sm
ψEO
0
5
10
15
20
25
DAI
F
Relative to control
110
100
90
80
70
60
Fv/Fm
Plabs
Sm
ψEO
0
5
10
15
20
25
DAI

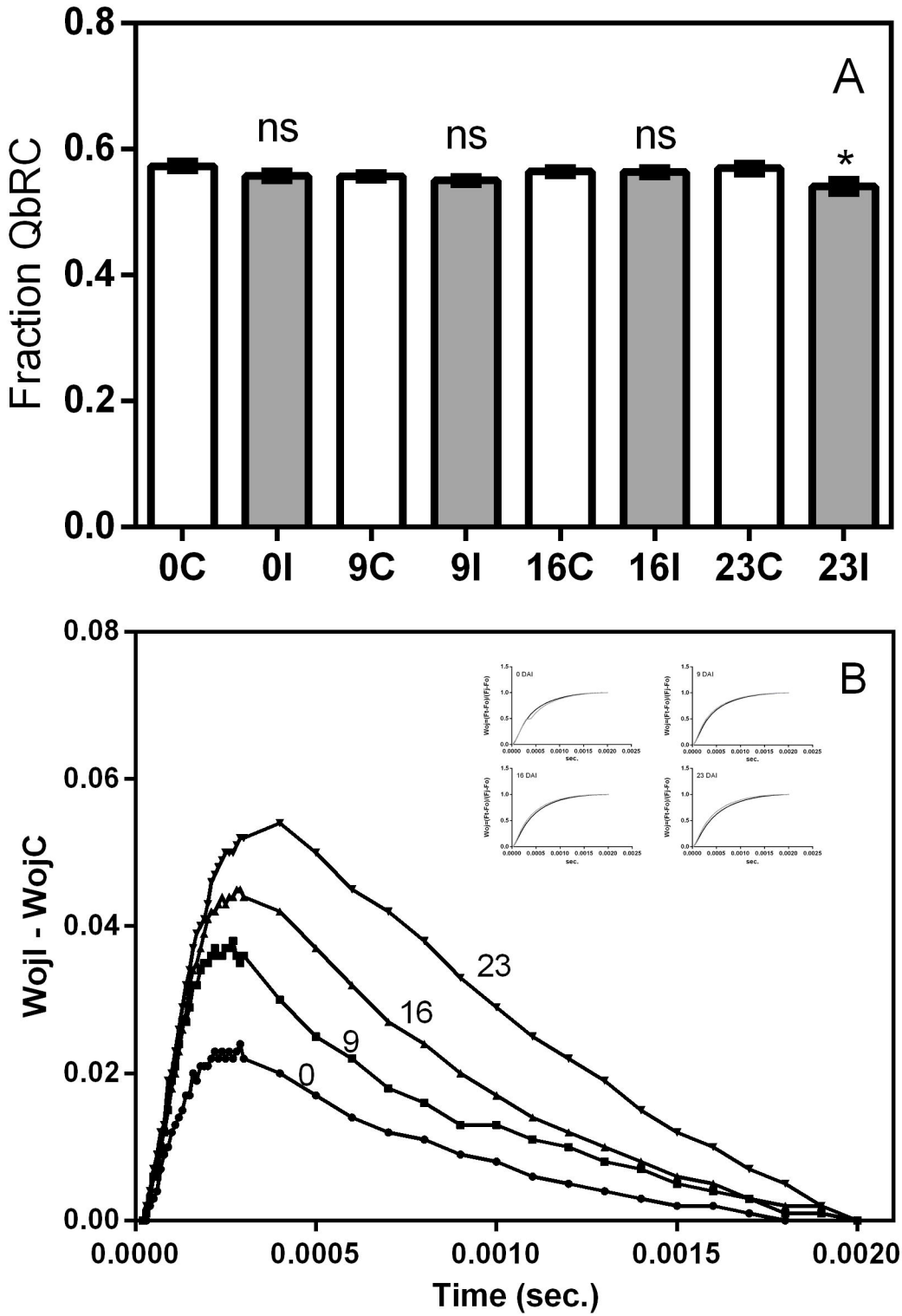
A
Fraction QbRC
0.0
0.2
0.4
0.6
0.8
ns
ns
ns
*
0C
0I
9C
9I
16C
16I
23C
23I
B
WojI - WojC
0.00
0.02
0.04
0.06
0.08
0.0000
0.0005
0.0010
0.0015
0.0020
Time (sec.)
23
16
9
0
0 DAI
9 DAI
16 DAI
23 DAI
sec.

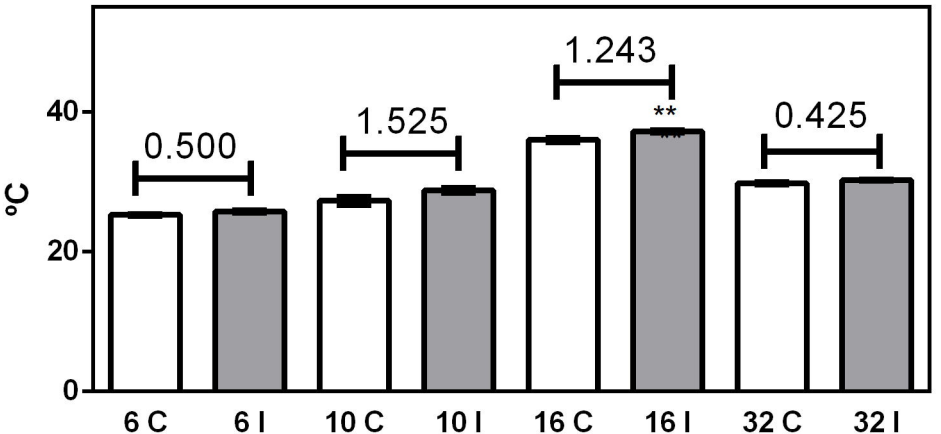
1.243
0.500
1.525
0.425
**
40
20
0
°C
6 C
6 I
10 C
10 I
16 C
16 I
32 C
32 I

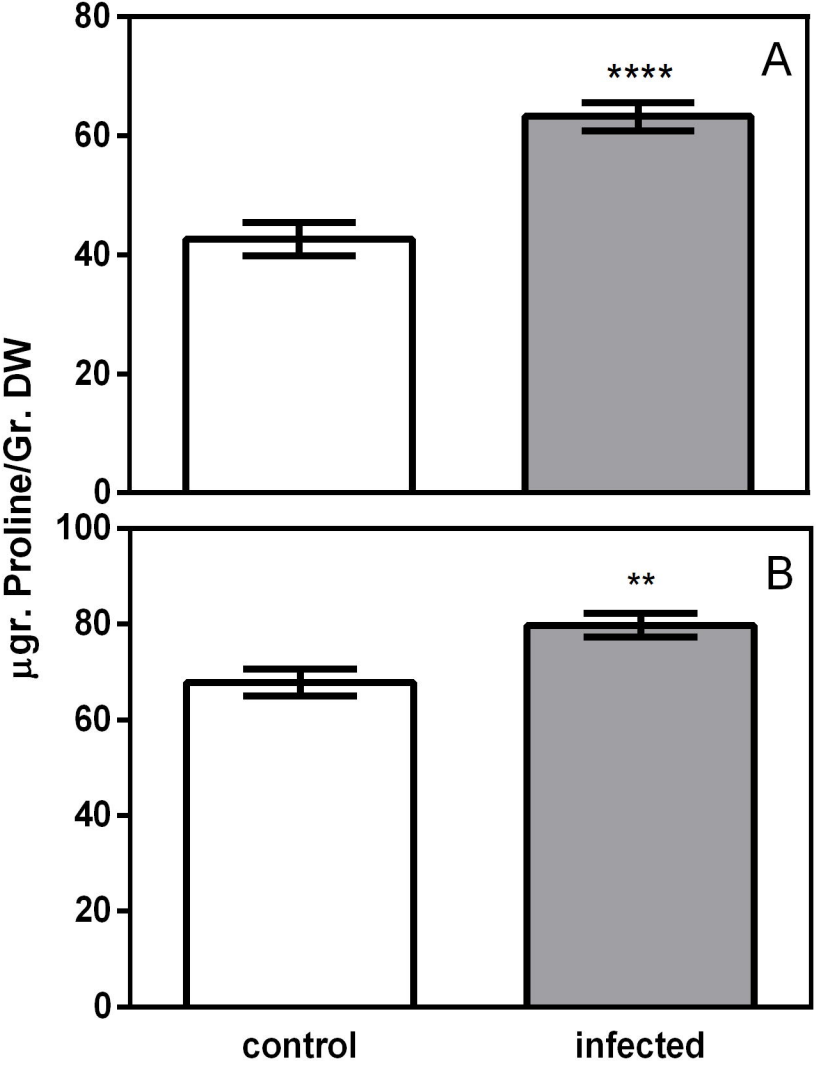
80
60
40
20
0
****
A
100
80
60
40
20
0
**
B
µgr. Proline/Gr. DW
control
infected